NS-FDTD 法と NTFF 変換を用いたサブ波長多層構造の反射スペクトル

朱 棟, 蔡 東生

筑波大学 システム情報工学研究科

要約: サブ波長多層構造はモルフォ蝶の鱗粉中の微細構造スケールに発見される。モルフォ蝶の青色発色はサブ波長多層構造に起因する。モルフォ蝶の青色を再現するためには、可視光範囲の構造の反射スペクトル分布が必要である。モルフォ蝶鱗粉多層構造に対する解析解は存在しない。本研究では、高精度非標準 FDTD（NS-FDTD）を用い、多層構造の近傍界を求める。そして、NTFF 変換を用いて近傍界を遠方界まで変換し、遠方界での反射強度を計算する。NS-FDTD と NTFF の計算を可視光の各波長で繰り返し、多層構造の反射スペクトルを算出し、モルフォ蝶の構造発色による青色を再現する BRDF を求める。

Reflection Spectrum of a Subwavelength Layered Structure Using NS-FDTD method and NTFF transformation

Dong Zhu, Dongsheng Cai
Dept. of Information Science, University of Tsukuba, Japan

Abstract: Subwavelength layered structures are found in the scales of Morpho butterfly. The iridescent blue color of the Morpho butterfly are mainly resulted from the subwavelength layered structures. To reproduce the coloring of Morpho butterflies, we need reflection spectrum of the structure in the range of visible light. Unfortunately, the analytical solution to the layered structures does not exist. Using a high-accuracy non-standard finite difference time domain (NS-FDTD) method, we calculated near field of the layered structure. Then applying near-to-far-field (NTFF) transformation on the near field, we computed reflected intensities on far field. Iterating the NS-FDTD-NTFF calculations with all wavelengths of visible light, we calculated reflection spectrum of the layered structure.

1. Introduction

The wings of Morpho butterfly have iridescent blue color. Four typical species of Morpho butterfly, M.rhetenor, M.sulkowskyi, M.didius and M.Adonis are shown in Fig.1. By scanning electron microscope (SEM), we can find that there are many scales shown in Fig.2(a) on the wings and dielectric layered structures shown in Fig.2(b) with subwavelength features in the scales. The coloring of Morpho butterfly is mainly originated from the subwavelength layered structure. This kind of coloring is called structural coloring. There are other examples of structural coloring in nature. Nowadays, structural coloring is applied in many fields.

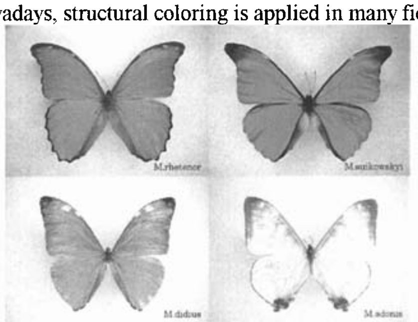

Fig. 1: Morpho butterflies, i.e. M.rhetenor, M.sulkowskyi, M.didius and M.Adonis

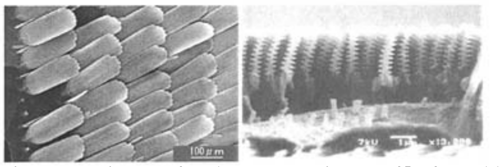

Fig. 2: SEM images of M.rhetenor. (a)A low-magnification SEM image of M.rhetenor. (b)A high-magnification SEM image of a cross-section through an M.rhetenor scale.

To reproduce the coloring of the Morpho butterfly, the reflection spectrum of the layered structure is needed. However, the analytical solution to the structure does not exist. In the Mie scattering regime, where feature size and wavelength are comparable, calculations of optical propagation are extremely difficult because scalar diffraction theory is invalid. Furthermore, analytic solutions exist only when the scatterer is highly symmetric or infinitely periodic.

Using a high accuracy nonstandard finite differences finite difference time domain (NS-FDTD) method [1] we compute the near field of the dielectric layered structure. The layered structure shown in Fig.3 is only an approximation of Morpho butterflies' layered structure. And then we use near-to-far-field (NTFF) transformation on the near field to calculate reflected intensities on far field. To test the NS-FDTD-NTFF method, firstly we use the method on the Mie scattering, because the Mie scattering has analytical solution and both the Mie scattering and the layered structure have subwavelength feature.

If given accurate result for the Mie scattering by the NS-FDTD-NTFF method, we use the method to calculate reflected intensities of the layered structure. Iterating the NS-FDTD-NTFF calculations with all wavelengths in visible light range, we compute reflection spectrum of the layered structure.

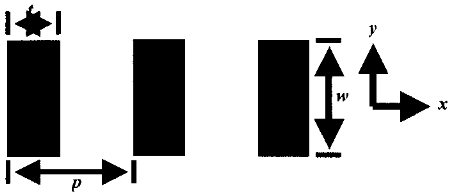

Fig.3. Layered Structure. Layer thickness t = 94nm, periodicity p = 235nm, width w = 329nm. There are 9 layers (not all shown). Dark area is dielectric material of refractive index n = 1.6.

2. NS-FDTD Method and NTFF transformation

We solve the Maxwell's equations in the non-conducting form

$$\mu \partial_t \boldsymbol{H} = -\nabla \times \boldsymbol{E}, \tag{1}$$

$$\varepsilon \partial_t \boldsymbol{E} = \nabla \times \boldsymbol{H}, \tag{2}$$

where the magnetic permeability μ is taken to be equal to the vacuum value everywhere, and the dielectric permittivity is normalized to be $\varepsilon = 1$ in vacuum and $\varepsilon = n^2$ within the dielectric. The normalized magnetic permeability μ is $\mu = 1/v_0^2$. An infinite plane wave $(\boldsymbol{E}_i, \boldsymbol{H}_i)$ impinges on the layered structure from the left along the x-axis (Fig.3). $(\boldsymbol{E}, \boldsymbol{H})$ is the sum of the incident and scattered electromagnetic fields, thus $(\boldsymbol{E}_s, \boldsymbol{H}_s) = (\boldsymbol{E}, \boldsymbol{H}) - (\boldsymbol{E}_i, \boldsymbol{H}_i)$. The incident fields obey Maxwell's equations assume vacuum were everywhere. Inserting $(\boldsymbol{E}_s, \boldsymbol{H}_s)$ into Eq(1) and Eq(2) yields

$$\mu \partial_t \boldsymbol{H}_s = -\nabla \times \boldsymbol{E}_s, \tag{3}$$

$$\varepsilon \partial_t \boldsymbol{E}_s = \nabla \times \boldsymbol{H}_s - (\varepsilon - 1)\partial_t \boldsymbol{E}_0. \tag{4}$$

The last term on the right of (4) is a source term that generates the scattered fields. It vanishes outside the scatterer where $(\varepsilon - 1) = 0$. An infinite plane wave is given by $\boldsymbol{E}_0 = \mathrm{Re}[\hat{\boldsymbol{p}} e^{i(\boldsymbol{k}\cdot \boldsymbol{x} - \omega t)}]$, where $\boldsymbol{k}$ is the wave vector, ω the angular frequency, and $\hat{\boldsymbol{p}}$ is a unit vector of the $\boldsymbol{E}_0$-direction. In the TE mode $\hat{\boldsymbol{p}} = \hat{z}$, and in the TM mode $\hat{\boldsymbol{p}} = \hat{y}$. The wave vector magnitude $k = |\boldsymbol{k}|$ is given by $\omega = vk$, where $v^2 = 1/\mu\varepsilon$.

The FDTD method (also called Yee algorithm) [2] is derived by replacing the derivatives with finite difference (FD),

$$\partial_x f(x,y) \cong d_x f(x,y)/h, \tag{5}$$

where d_x is a difference operator defined by $d_x f(x) = f(x + h/2, y) - f(x - h/2, y)$. Defining $\boldsymbol{d} = (d_x, d_y, d_z)$, we have $\nabla \times \cong \boldsymbol{d} \times / h$, where we have taken $\Delta x = \Delta y = \Delta z = h$. The FDTD method for (3) and (4) becomes

$$\boldsymbol{H}_s(\boldsymbol{x}, t + \Delta t/2) = \boldsymbol{H}_s(\boldsymbol{x}, t - \Delta t/2) - \frac{\Delta t}{\mu h} \boldsymbol{d} \times \boldsymbol{E}_s(\boldsymbol{x}, t), \tag{6}$$

$$\boldsymbol{E}_s(\boldsymbol{x}, t + \Delta t) = \boldsymbol{E}_s(\boldsymbol{x}, t) + \frac{\Delta t}{\varepsilon h} \boldsymbol{d} \times \boldsymbol{H}_s(\boldsymbol{x}, t + \Delta t/2) - (\varepsilon(\boldsymbol{x}) - 1)\partial_t \boldsymbol{E}_0(\boldsymbol{x}, t + \Delta t/2), \tag{7}$$

where $\boldsymbol{x} = (x, y, z)$. In the ordinary FDTD method, the error in the finite difference approximation (5) is $\varepsilon \sim (h/\lambda)^2$.

In the NS-FDTD method we modified Eq(6) by replacing $v\Delta t/h \to u$, Eq(7) $v\Delta t/h \to u$ and $\boldsymbol{d} \to \boldsymbol{d}_0$, where $u = \sin(\omega\Delta t/2)/\sin(kh/2)$, and $\boldsymbol{d}_0$ is a new composite difference operator, which is formed by superposing three independent finite differnce operators for ∇, as described in [1]. The NS-FDTD method for (3) and (4) becomes

$$\boldsymbol{H}_s(\boldsymbol{x}, t + \Delta t/2) = \boldsymbol{H}_s(\boldsymbol{x}, t - \Delta t/2) - \frac{\Delta t}{\mu h} \boldsymbol{d} \times \boldsymbol{E}_s(\boldsymbol{x}, t), \tag{8}$$

$$\boldsymbol{E}_s(\boldsymbol{x}, t + \Delta t) = \boldsymbol{E}_s(\boldsymbol{x}, t) + \frac{\Delta t}{\varepsilon h} \boldsymbol{d} \times \boldsymbol{H}_s(\boldsymbol{x}, t + \Delta t/2) - (\varepsilon(\boldsymbol{x}) - 1)\partial_t \boldsymbol{E}_0(\boldsymbol{x}, t + \Delta t/2). \tag{9}$$

In the NS-FDTD method the error is reduced to $\varepsilon \sim (h/\lambda)^6$.

In our NS-FDTD simulation, all parameters are normalized. The wavelength in the simulation λ_0 is the ratio λ/h ,where λ is physical wavelength and h is physical cellsize. The magnetic permeability μ is taken to be $\mu = 1/v_0^2$ everywhere. The dielectric permittivity is normalized to be $\varepsilon = 1$ in vacuum and $\varepsilon = n^2$ within the dielectric. The velocity in vacuum v_0 is also normalized. For the NS-FDTD method v_0 must satisfy $v_0 < 0.83$ [1]. To determine the cellsize h ,we run the NS-FDTD simulation from some cellsize and does not make the cellsize smaller until the angular intensity distribution converges.

After the near field stabilizes, we use the NTFF transformation to compute the far field. The formulas of the two-dimensional NTFF transformation [3] are

$$\boldsymbol{E}_\phi = -z_0 \boldsymbol{N}_\phi - \boldsymbol{L}_z,$$

$$\boldsymbol{E}_z = -z_0 \boldsymbol{N}_z + \boldsymbol{L}_\phi,$$

where

$$N(\omega)=\sqrt{\frac{j\omega}{8\pi cr}}e^{jkr}\int_c Js(\omega,r')\exp(jk\hat{r}\cdot r')ds',$$

$$L(\omega)=\sqrt{\frac{j\omega}{8\pi cr}}e^{jkr}\int_c Ms(\omega,r')\exp(jk\hat{r}\cdot r')ds',$$

where $Js=\hat{n}\times H$, $Ms=E\times\hat{n}$, $\hat{r}$ is the unit vector to the far field point, r' is the vector to the source point of integration, r is the distance to the far field point, and c is a closed curve surrounding the scatterer.

3. Experiments and results

Light scattering is very important in structure coloring. When the size of particle is comparable with the wavelength of light source, it is called Mie scattering. Analytical solution of the Mie scattering has been worked out. Thus, firstly we use the NS-FDTD-NTFF method on Mie scattering, and compare the computational results with the analytical solutions.

We made a 60×60 numerical grid and set up a dielectric cylinder $r=0.75\lambda_0$ and $n=1.6$ on numerical grid shown in Fig.4. The normalized wavelength λ_0 is taken to be $\lambda_0=8$. Since the cellsize is set to be 50nm, $\lambda_0=8$ means physical wavelength $\lambda=400nm$.

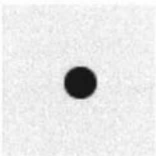

Fig.4. cylinder structure of the Mie scattering. The black area is a dielectric cylinder.

An infinite plane wave is incident from the left upon the dielectric cylinder. Near fields of TE and TM mode are calculated using the NS-FDTD method and compared with analytical solutions shown in Fig.5 and Fig.6. As we can see, the NS-FDTD method gives much better result than FDTD.

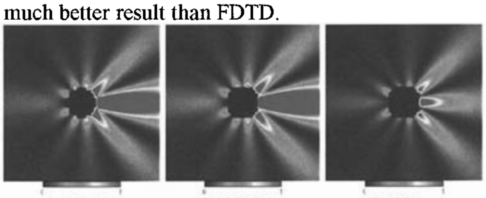

Fig.5 visualization of $|E_z|^2$ of Mie scattering for TM mode.

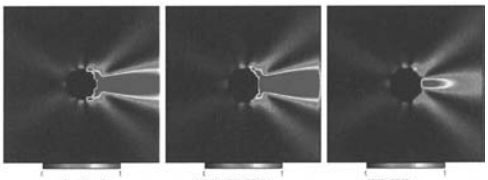

Fig.6 visualization of $|E_y|^2$ of Mie scattering for TE mode.

The scattered intensities on far fields of TE mode and TM mode at the distance $r=1000\lambda_0$ are calculated from the near field using NTFF. The analytical solution, computational results from NS-FDTD's near field and FDTD's near field are plotted as a function of scattering angle in Fig.7 and Fig.8.

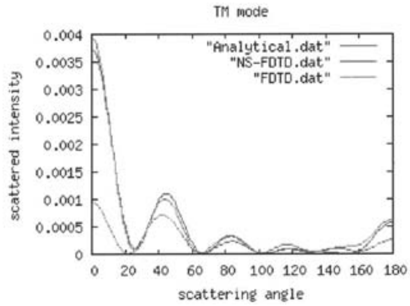

Fig.7. Far field scattered intensity of the Mie scattering of TM mode.

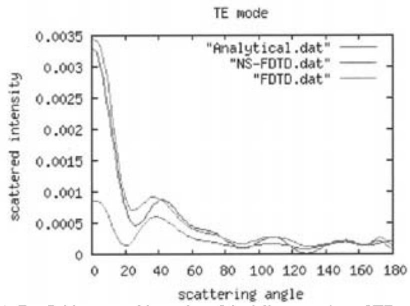

Fig.8. Far field scattered intensity of the Mie scattering of TE mode.

Comparing with analytical solution in Fig.7 and Fig.8, we can find that NS-FDTD-NTFF method gives highly accurate solution for wavelength $\lambda=400nm$. Then we can go to test all wavelengths in the 400nm-700nm range. We calculated the scattering spectrum and compared it with analytical solution. From Fig.9 and Fig.10, we can see that the result by NS-FDTD-NTFF method is much closer to analytical solution, because NS-FDTD method gives much more accurate near field than FDTD method.

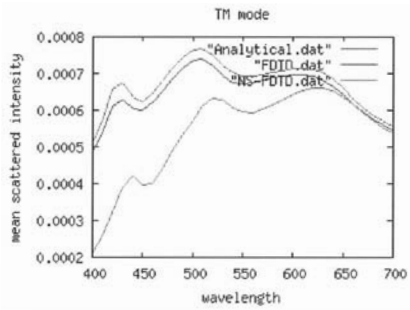

Fig.9 Mean scattered intensity ($0\text{-}180^\circ$) of the Mie scattering in the TM mode as a function of wavelength.

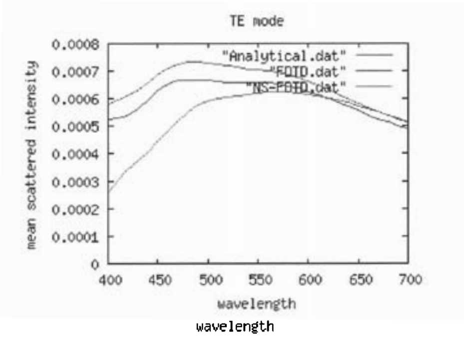

Fig.10 Mean scattered intensity ($0\text{-}180^{\circ}$) of the Mie scattering in the TE mode as a function of wavelength.

The NS-FDTD-NTFF method gives high accuracy for the Mie scattering. Then we can use the method to the layered structure, because both the Mie scattering and the layered structure have subwavelength feature. We investigate reflection spectrum of the layered structure in the 400 -700nm wavelength range by the NS-FDTD-NTFF method. The layered structure is shown in Fig.10. The grid size is taken to be 100×100. In the same way, an infinite plane wave is incident from the left upon the layered structure. The near fields of TE and TM mode are calculated with NS-FDTD method. The far field is calculated at the distance $r = 1000\lambda_0$ using the NTFF transformation. The far fields with the reflective angle from 0° to 180° of some wavelengths are plotted in Fig.11 and Fig.12. Iterating the NS-FDTD and NTFF for all wavelengths in 400 -700nm range, we calculated the reflection spectrum of the layeres structure.

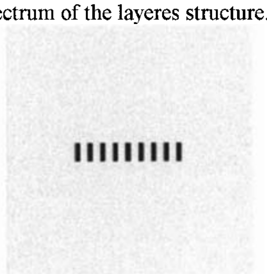

Fig.10. Finite layered structure. Layer thickness $t = 94$nm, periodicity $p = 235$nm, width $w = 329nm$. Dark area is dielectric material of refractive index $n = 1.6$. Gray area is vacuum with $n = 1.0$.

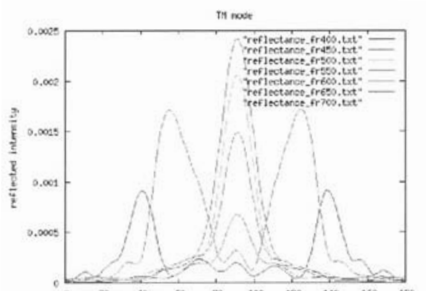

Fig.11 angular reflected intensity of the layered structure(TM mode).

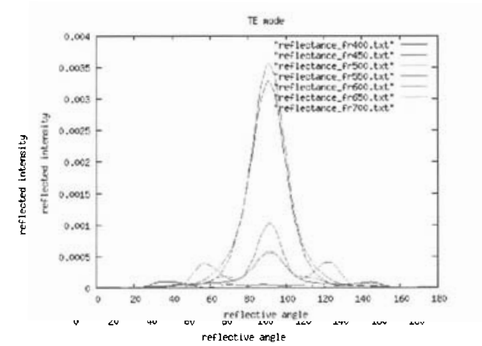

Fig.12 angular reflected intensity of the layered structure(TE mode).

From the Fig.11 and Fig.12, we can see that the reflected intensities of some wavelengths are quite sensitive to reflective angles. For TM mode, below 500 nm the edges of the layered structure give rise to diffraction peaks at increasing angle, while at longer wavelengths, the reflectance is large near 90° and falls quickly with increasing angle. Around 500nm, the reflectance reaches the maximum. After 500nm, it gradually falls with increasing wavelength. For TE mode, the wavelength of the reflection maximum moves to 550nm and near 500nm to 550nm the reflectance is much larger than other wavelengths.

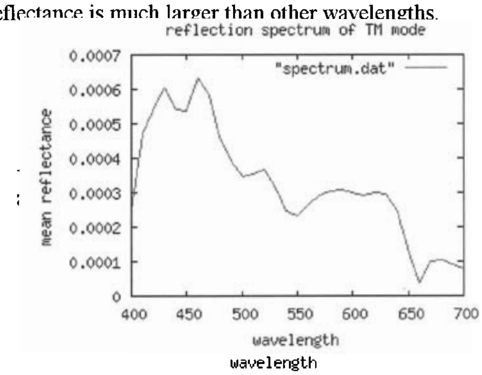

Fig.13. Mean scattered intensity ($0\text{-}180^{\circ}$) of the layered structure for TM mode

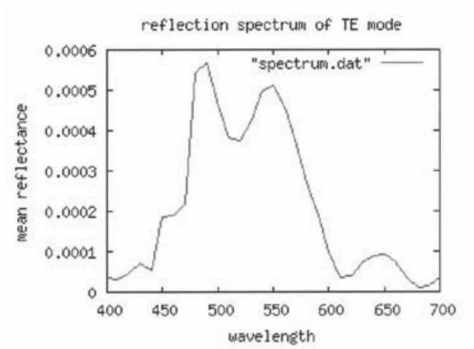

Fig.14. Mean scattered intensity ($0\text{-}180^{\circ}$) of the layered structure for TE mode

The reflection spectrum is plotted in Fig.13 and Fig.14. For TM mode, most of the reflection is located from 420nm to 550nm, while for TE mode from 480nm to 580nm.

4. Conclusion and future work

We investigated reflection spectrum of a subwavelength layered structure using NS-FDTD-NTFF method. The subwavelength layered structure we calculated is just an approximation of the Morpho butterflies' structure. And we just calculated one layered structure and have not considered the affection between two neighboured structures. Later, we are going to investigate a set of several layered structures closer to the Morpho butterflies' structure.

5. References

1) J. B. Cole, S. Banerjee, and M. Haftel: Chapter in "Advances in the Applications of Nonstandard Finite Difference Schemes," R. E. Mickens, ed., World Scientific (Singapore, 2005).

2) K. S. Kunz and R. J. Luebbers, "The Finite Difference Time Domain Method for Electromagnetics" CRC Press, New York (1993).

3) Raymond Luebbers, Deirdre Ryan, and John Beggs "A Two-Dimensional Near-Zone to Far-Zone Transformation" p848-851, IEEE Transactions on Antennas and Propagation, VOL 40, No.7, July 1992